





ORIGINAL ARTICLE OPEN ACCESS

Comparison of Healing Outcomes Between Simultaneous and Staged Implant Placement With Sinus Floor Elevation: A Preclinical Study Using a Rabbit Sinus Model

Ji-Youn $\operatorname{Hong^1} \bigcirc$ | Yeek $\operatorname{Herr^1}$ | Nadja Naenni² | Daniel S. Thoma²,³ \bigcirc | Borvornwut Buranawat⁴ | Seung-Il Shin¹ | Hyun-Chang $\operatorname{Lim}^{1,2,4} \bigcirc$

¹Department of Periodontology, Kyung Hee University College of Dentistry, Periodontal-Implant Clinical Research Institute, Kyung Hee University Medical Center, Seoul, Republic of Korea | ²Clinic of Reconstructive Dentistry, University of Zurich, Zurich, Switzerland | ³Department of Periodontology, Yonsei University College of Dentistry, Seoul, Republic of Korea | ⁴Center for Implant Dentistry and Periodontics, Faculty of Dentistry and Research Unit in Innovations in Periodontics, Oral Surgery and Advanced Technology in Implant Dentistry, Thammasat University, Pathum Thani, Thailand

Correspondence: Hyun-Chang Lim (periodent81@gmail.com)

Received: 28 March 2025 | Revised: 15 July 2025 | Accepted: 11 August 2025

Funding: This work was partially supported by the alumni association (KPERIO) of the Department of Periodontology, Kyung Hee University College of Dentistry, Seoul, Korea.

Keywords: animal model | bone regeneration | dental implant | sinus floor augmentation

ABSTRACT

Aim: To compare the histological healing between implants placed simultaneously with maxillary sinus floor augmentation (MSFA) and those placed with a staged approach in the maxillary sinus with thin bone height.

Materials and Methods: MSFA was performed on both sides of the sinuses in 10 rabbits, followed by simultaneous implant placement in one of the sinuses (group SMT). Four weeks later, implant placement was performed in the other sinus (group STG). The animals were euthanised 8 weeks thereafter. Micro-computed tomographic and histomorphometric analyses were performed. **Results:** In micro-computed tomographic images, the implants were well surrounded by newly formed bone (NB) and bone substitute particles, without statistically significant difference in the volume of NB between the groups (p > 0.05). Histomorphometrically, the amount of NB within the total augmented area and ROIs near the implants did not significantly differ between the groups (p > 0.05). The percentage of bone-to-implant contact was not significantly different between the groups ($52.2\% \pm 16.6\%$ vs. $44.9\% \pm 18.4\%$; p > 0.05).

Conclusions: Simultaneous implant placement with MSFA resulted in comparable radiographic and histological outcomes to a staged implant placement approach in sinuses with thin bone height. However, such outcomes should be cautiously interpreted within the context of an animal model.

1 | Introduction

Residual bone height (RBH) in the posterior maxilla has been regarded as a primary determinant for implant placement modality (either simultaneously with or following maxillary sinus floor augmentation [MSFA]) (Jensen et al. 1998). According to these guidelines, multiple surgeries should be planned for the posterior

maxilla with low RBH, for instance, start with a lateral maxillary sinus floor elevation (MSFA) to create adequate bone height. This should be followed by implant placement using a submerged healing technique and, finally, the abutment connection (uncover procedure). Such an approach guarantees safety (Corbella et al. 2015; Del Fabbro et al. 2013; Wallace and Froum 2003), but at the same time, increases treatment time, patient morbidity and costs.

This is an open access article under the terms of the Creative Commons Attribution-NonCommercial-NoDerivs License, which permits use and distribution in any medium, provided the original work is properly cited, the use is non-commercial and no modifications or adaptations are made.

© 2025 The Author(s). Journal of Clinical Periodontology published by John Wiley & Sons Ltd.

Whether RBH remains a primary determinant leaves room for a revisit. It was speculated that the thinner the RBH, the fewer the osteogenic sources available, which was based on the biological expectation that the cancellous bone part is a stronger donor of osteogenic sources (Corbella et al. 2016). Moreover, human biopsy studies had shown that less new bone is formed as the distance from the native bone increases (Beck et al. 2021; Pignaton et al. 2020). Thus, the bone-to-implant contact (BIC) ratio might be smaller at implants placed in sinuses with thin RBH than thicker RBH.

On the other hand, other clinical studies have shown that RBH was not related to new bone formation in the augmented sinuses even though different threshold values for RBH were employed to compare the bone formation in those studies (≤ 4 mm, ≥ 4 mm/ ≤ 4 mm, > 2 mm/ ≤ 2 mm) (Avila-Ortiz et al. 2012; Pignaton et al. 2019; Zhou et al. 2021). Furthermore, the anatomical structure of the maxillary sinus, which is surrounded by bone walls, inherently supports intra-sinus bone formation. Therefore, the impact of RBH on new bone formation may not be as significant as previously thought.

Surgical difficulty and predictability of the treatment for MSFA with thin RBH may vary depending on the applied technique and materials. Earlier studies had shown that implant survival in the posterior maxilla was lower when RBH was ≤4mm (Rosen et al. 1999). However, many factors related to MSFA (implant type, graft material, surgical instruments and understanding of the MSFA procedure) have improved since then. This allows revisiting these procedures. Indeed, old implant surfaces are not used anymore in clinical settings. A systematic review revealed that modern implant surfaces yielded higher implant survival in the augmented sinus (Del Fabbro et al. 2008). Moreover, improvements in implant design and surgical techniques provide better primary stability (Abuhussein et al. 2010; Jamil 2024; Tabassum et al. 2010). Indeed, some recent studies have shown several positive outcomes of the implant placed simultaneously with MSFA at the posterior maxilla with thin RBH (Liu et al. 2022; Virnik et al. 2023).

Despite growing evidence, there is currently no data directly comparing implants placed simultaneously with MSFA and staged implant placement following MSFA. Osseointegration of implants placed in sites with a thin RBH heavily depends on the augmented area (sinus) rather than the residual native bone. Available clinical studies do not sufficiently reflect these aspects for the following reasons: (i) lack of or insufficient histological analysis (limited to a core biopsy), and (ii) histological specimens obtained prior to implant placement and not encompassing the implant within the augmented sinus (staged approach) (Avila-Ortiz et al. 2012; Kim et al. 2020; Pignaton et al. 2019). Therefore, investigating the histological peri-implant healing in the presence of a thin RBH in a preclinical model is essential to translate the data into a clinical setting. A preclinical model allows more detailed histological and radiographic evaluations-which are not obtainable in clinical research—such as BIC and spatial periimplant healing patterns.

The present preclinical study aimed to compare the healing outcomes between implants placed simultaneously and those staged with MSFA in sinuses with thin RBH.

2 | Materials and Methods

The study protocol was approved by the Institutional Animal Research Committee at Kyung Hee Medical Center, Seoul, Korea (KHMC-IACUC 2022–038), and followed the ARRIVE guidelines 2.0 (Percie du Sert et al. 2020).

2.1 | Animals

Ten male, adult New Zealand white rabbits (weighing 2.5–3.0 kg, 12 months old) were used. Appendix 1 contains the information regarding animal care and handling.

2.2 | Study Groups

- Group SMT: simultaneous implant placement with MSFA;
- · Group STG: staged implant placement after MSFA.

MSFA in both groups and implant placement in group SMT were performed in the same surgical session. After 4 weeks, implant placement was performed in group SMT. This was followed by 8 weeks of healing.

2.3 | Outcome Measures

2.3.1 | Primary Outcome

 Bone-to-implant contact ratio (%BIC), assessed through histomorphometric analysis.

2.3.2 | Secondary Outcomes

- Areas of newly formed bone (NB), residual bone substitute material (RM) and fibrovascular tissue (FV) within the entire augmentation and regions of interest (ROIs) assessed through histomorphometric analysis;
- · Antral bone thickness;
- Percentage of implant engagement to the antral bone;
- Volumes of NB and RM within entire augmentation and ROIs, assessed in micro-computed tomography (micro-CT) scan.

2.4 | Surgeries

2.4.1 | Surgery 1 (For Both Groups)

Mid-sagittal incision was performed along the midline of the antral area, followed by reflecting a full-thickness flap. A specially designed sinus drill system (Shinhung, Seoul, Korea) was used to prepare a bony access window in both groups. The final diameter of the access window was 3.7 mm. Subsequently, the sinus membrane was detached from the adjacent bone using a sinus curette (Dentium, Seoul, Korea) and hydraulic pressure by saline injection (Lee et al. 2022; Sim et al. 2022). After confirming

sufficient sinus membrane elevation anteriorly to the access window, a standardised amount (0.25 mL) of synthetic bone substitute material (Osteon3, Genoss, Suwon, Korea) was grafted. In the group SMT, sequential drilling was performed for implant placement according to the manufacturer's guidelines. During drilling, a surgical curette was inserted into the window to protect against inadvertent damage to the sinus membrane. The final osteotomy was $1.0-1.5\,\mathrm{mm}$ away from the access window. An implant was placed manually (Bright implant $\emptyset 3.0 \times 7.0\,\mathrm{mm}$, Dentium), and a cover screw was connected to the implant. The implant had a 2-mm polished collar. Thus, 5 mm of the rough surface was embedded into the antral bone and augmented area in the sinus, resulting in an exposure of 2 mm above the antral bone (Figure 1). The flaps were sutured (4–0 Monosyn, B. Braun, Aesculap, PA, USA). The sutures were removed after 1 week.

2.4.2 | Surgery 2 (For Group STG)

After 4weeks, the flap was reflected to expose the antral bone part. An implant was placed in the same cephalo-caudal position as in group SMT. After connecting a cover screw to the implant, the flaps were sutured. The sutures were removed after 1 week.

2.4.3 | Sacrifice

At 8 weeks following the surgery 2, all animals were first anaesthetised and euthanised by an intra-cardiac injection of urethane (ethyl carbamate, 4g/10 mL; Sigma–Aldrich, St Louis, MO, USA).

2.5 | Micro-CT Analysis

The harvested specimens were immersed in 10% neutral buffered formalin. Prior to processing the specimen for histological processing, micro-CT was performed (SkyScan 1173 ver. 1.6; Bruker-MicroCT, Kontich, Belgium) with the following conditions: 130 kV, $60\,\mu\text{A}$, pixel size=29.9 μm , exposure=500 ms. The obtained images were reconstructed using NRecon software (ver. 1.7.4.6; Bruker Micro-CT).

Two ROIs were established. The first ROI (ROI_1) was the total augmented dimension with the exclusion of the implant. The

second ROI (ROI $_2$) was a circular band around the implant between 60 and 375 μ m from the implant surface and an alternative to BIC (Diefenbeck et al. 2011; He et al. 2017; Maniatopoulos et al. 1986) (Appendix 1). Total augmented volume (TV; mm³) as well as the volumes of newly formed bone (NV; mm³) and the residual bone substitute material (RV; mm³) were measured in ROI $_1$. In ROI $_2$, NV and RV were measured.

2.6 | Histological and Histomorphometric Analyses

After micro-CT, histological slides were produced from the retrieved specimens (Appendix 1), followed by digital scanning and analyses using the computer software SlideViewer ver. 2.5 (3DHISTECH, Budapest, Hungary) and Photoshop 2024 (Adobe, CA, USA).

The initial analysis included the following parameters: (i) total augmented area (TA, mm²): the area surrounded by the access window, the sinus membrane and the surrounding bone walls, excluding the implant; (ii) the area of newly formed bone within TA (NB, mm²); (iii) area of the residual bone substitute material within TA (RM, mm²); and (iv) area of fibrovascular tissue within TA (FV, mm²) (Figure 2). Then, two ROIs were established in the area close to the implant. The first ROI (ROI,) was defined as 1 mm away from the axial surfaces of the implant body core, 0.5 mm away from the implant bottom, and the line along the rough/smooth border of the implant. The second ROI (ROI₂) was defined as the areas between the implant threads (Figure 2). For these two ROIs, the same parameters (as the above) were measured: TA ROI, NB ROI, RM ROI and FV ROI (mm²). These parameters were calculated as percentages in the respective areas (TA or TA_ROI) because of their different dimensions.

Moreover, the thickness of the antral bone on both lateral sides of the implant was measured and averaged. Then, the percentage of implant engagement to the antral bone was calculated.

Finally, %BIC (primary outcome) was measured within the rough surface at the lateral sides of the implant. In measuring %BIC, the contact with the native antral bone was excluded.

Training and calibration of the examiners are shown in Appendix 1.

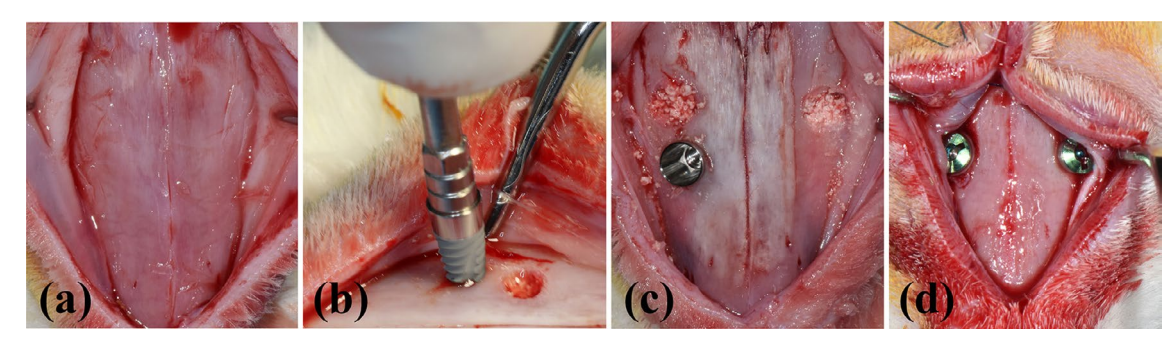


FIGURE 1 | Clinical photographs of surgical procedures. (a) A full-thickness flap was elevated to expose the antral bone surface. (b) After bone grafting in both sinus cavities, implant osteotomy was performed on one side of the sinus, followed by placing the implant manually. (c) After simultaneous implant placement and maxillary sinus floor augmentation (MSFA) in group SMT and after MSFA in group STG. (d) After implant placement in group STG (at 4 weeks post MSFA).

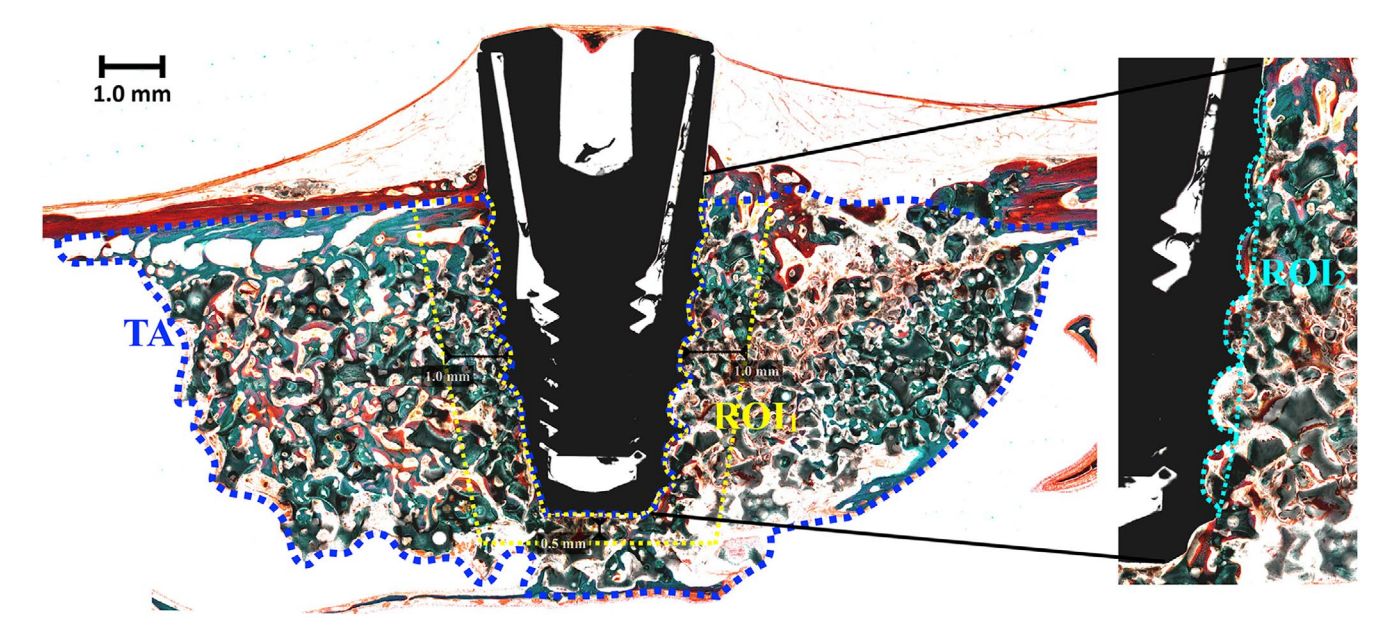


FIGURE 2 | Histomorphometric measurement.

Group SMT

Group STG





FIGURE 3 | Representative micro-computed tomography images of groups SMT and STG.

2.7 | Statistical Analyses

The sample size in the present study was arbitrarily determined to be 10 animals, based on the study by Thoma et al. (2018) (Appendix 1).

Statistical analyses were performed using SPSS software (version 21.0, SPSS, Chicago, IL, US). Data are presented as mean with standard deviation, median and interquartile range (IQR). Shapiro–Wilk tests were performed for checking conformity with normal distribution. After confirming that all parameters were normally distributed, parametric paired t-tests were applied for determining statistically significant inter-group differences. The level of statistical significance was set at p < 0.05.

3 | Results

3.1 | Clinical Finding

During MSFA and implant placement, no sinus membrane perforation was detected. All implants were clinically stable after the surgery. There was no rotation or vertical mobility.

The healing was uneventful in all animals. During the preparation of the tissue specimens, all implants were well integrated. No displacement or non-integration of implants was found.

3.2 | Micro-CT Analysis

The augmented sinuses were dome-shaped. The rough surface of the implants was well surrounded by newly formed bone and bone substitute particles in all specimens. No radiolucency was found in the proximity of the implants. In some specimens, the implant apex partially protruded into the sinus without being surrounded by hard tissue (Figure 3).

In ROI₁, there were no statistically significant differences in TV, NV or RV between groups SMT and STG (p < 0.05). In ROI₂, NV (4.1 \pm 1.1 mm³ vs. 3.8 ± 1.2 mm³) and RV also did not show any significant differences between the groups (p < 0.05) (Table 1).

3.3 | Histological Observations

The histological pattern of bone formation did not show any distinct differences between the two groups. The native antral bone

had smoothly transitioned into newly formed bone. The amount of newly formed bone in the middle of the augmentation looked smaller than in the areas near the antral bone and the sinus membrane in both groups. Bone apposition was observed on the rough surface of the implants to varying degrees. The middle part of the implants was in less contact with newly formed bone compared to the coronal and apical parts. In some implants, the apical part of the implant was partially covered with the sinus membrane (Figure 4).

TABLE 1 | Micro-computed tomographic outcomes.

	Group SMT	Group STG	p
ROI_1			
$TV (mm^3)$	248.9 ± 30.0	253.0 ± 25.5	0.666
$NV (mm^3)$	71.1 ± 6.8	71.4 ± 4.1	0.879
$RV (mm^3)$	56.4 ± 8.8	57.0 ± 9.3	0.723
%NV	28.7 ± 2.4	28.5 ± 3.4	0.813
%RV	22.8 ± 3.2	22.7 ± 3.9	0.931
ROI_2			
$NB (mm^3)$	4.1 ± 1.1	3.8 ± 1.2	0.192
$RV (mm^3)$	3.1 ± 0.7	3.1 ± 0.7	0.547

Note: Data are mean ± standard-deviation.

Abbreviations: %NV, percentage of newly formed bone in the respective region; %RV, percentage of residual bone substitute material in the respective region; NV, volume of newly formed bone; RV, volume of residual bone substitute material; TV, total augmented volume.

3.4 | Histomorphometric Analyses

3.4.1 | Entire Augmentation

The values of TA were $47.6\pm6.9\,\mathrm{mm^2}$ and $48.8\pm8.6\,\mathrm{mm^2}$ in groups SMT and STG, respectively (p>0.05). NB was slightly smaller in group SMT $(7.4\pm1.8\,\mathrm{mm^2})$ than in group STG $(8.0\pm1.9\,\mathrm{mm^2})$ (p>0.05). Significantly less RM was measured in group STG $(14.4\pm2.9\,\mathrm{mm^2})$ compared to group SMT $(16.1\pm1.8\,\mathrm{mm^2})$ (p<0.05). The %NB and %RM were not statistically significantly different between the groups (p>0.05) (Table 2; Figure 5).

3.4.2 | Region of Interest 1

The area of ${\rm ROI}_1$ was not statistically significantly different between the two groups (p>0.05). There was no statistically significant difference between the two groups regarding the absolute and percentage values of NB $(1.9\pm0.5~{\rm vs.}~1.7\pm0.4~{\rm mm}^2;$ $19.8\%\pm6.6\%~{\rm vs.}~18.6\%\pm5.8\%)$ and RM (p>0.05) (Table 2; Figure 5).

3.4.3 | Region of Interest 2

No statistically significant differences were noted in the area of ROI $_2$, NB (0.2±0.1 vs. 0.2±0.1 mm 2), RM and also %NB (25.9%±9.2% vs. 21.8%±13.2%) and %RM (p>0.05) (Table 2; Figure 5).

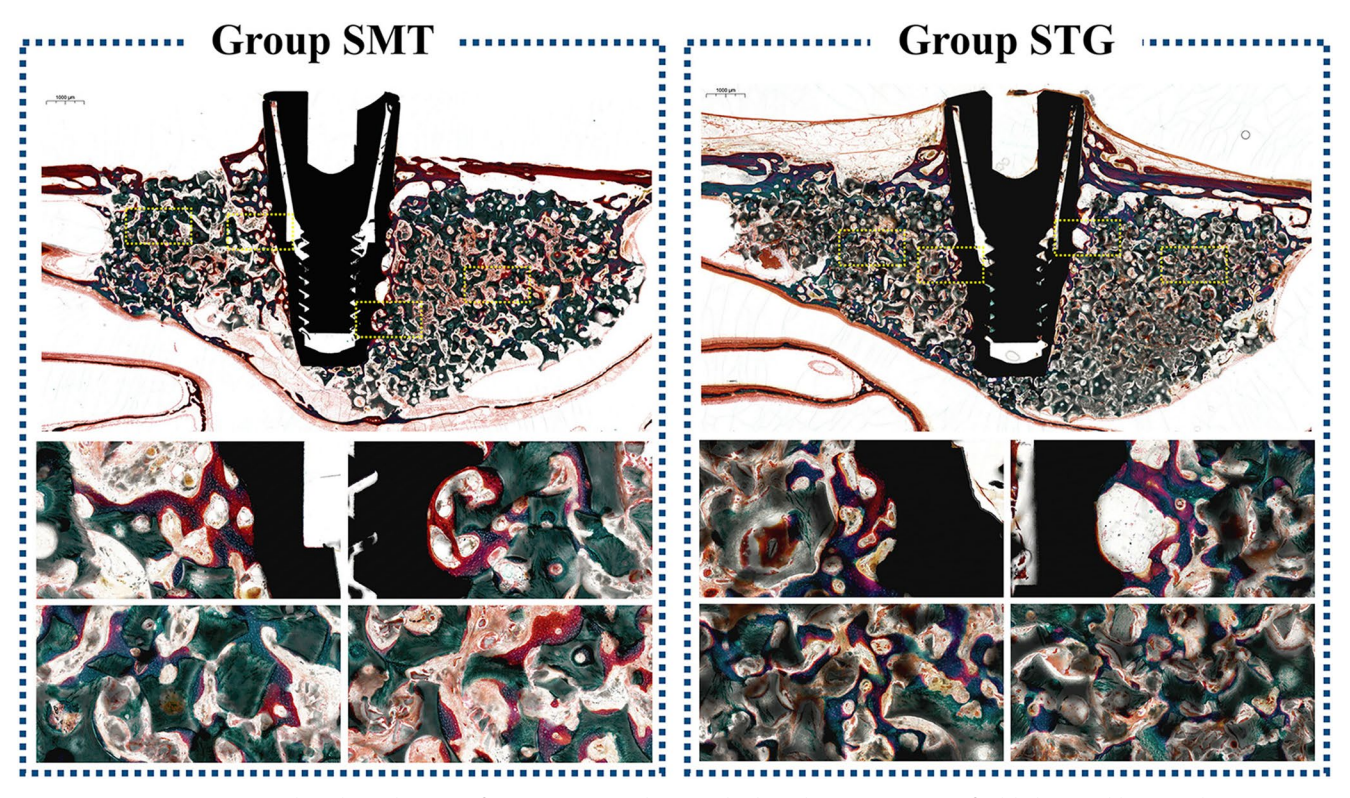


FIGURE 4 | Representative histological views of groups SMT and STG. The boxed areas are magnified below. Goldner Trichrome staining. Asterisk and triangle indicate newly formed bone (NB) and residual bone substitute material (RM), respectively.

3.4.4 | Percentage of Bone-To-Implant Contact

%BIC in group SMT (52.2% \pm 16.6%) was higher than in group STG (44.9% \pm 18.4%) without reaching statistical significance (p > 0.05) (Table 1).

4 | Discussion

4.1 | Summary of Findings

The present study investigated the effect of the timing of implant placement with respect to MSFA for sinuses with thin RBH in a rabbit sinus model. Key findings were as follows: (i) The timing of implant placement did not influence new bone formation in the vicinity of the implants and the augmented sinus in general. (ii) simultaneous implant placement does not negatively impact osseointegration.

4.2 | Micro-CT and Histomorphometric Findings

Traditionally, the timing of implant placement in the pneumatised posterior maxilla is determined primarily by the available RBH. Consequently, sites with thin RBH typically require multiple and more invasive surgical procedures. However, several studies have provided data for revisiting these approaches (Bernardello et al. 2011; Gonzalez et al. 2014; Liu et al. 2022; Virnik et al. 2023), suggesting that simultaneous implant placement with MSFA can be a viable option even in the posterior maxilla with thin RBH under certain conditions.

In the present study, micro-CT and histomorphometric analyses were performed at various levels to scrutinise bone formation: that is, the entire augmentation and specific regions close to the implant surface. Different baselines were conditioned into two groups (groups SMT and STG) in terms of osseointegration. In group SMT, the implant surface initially faced mostly bone substitute particles and the blood coagulum, whereas in group STG, the surface came in contact with the composite of newly formed bone, bone substitute particles and matrix tissues. It was anticipated that there would be close contact between the bone tissues and the implant surface in group STG at the time of implant placement. Given these different baselines, it was initially assumed that healing near the implant—particularly in ROI₂ (in both micro-CT and histomorphometric analyses) and %BIC—might differ from that in areas in ROI, and the entire augmentation.

However, the micro-CT and histomorphometric analyses in the present study revealed no significant differences in new bone formation at all analysed regions. This indicates that simultaneous implant placement with MSFA may not jeopardise osseointegration, even in sites exhibiting thin RBH. It is generally believed that RBH plays a pivotal role in endo-sinus bone formation after MSFA. However, sporadically published studies showed the opposite findings (Avila-Ortiz et al. 2012; Kim et al. 2020; Pignaton et al. 2019; Virnik et al. 2023). In some of those studies, MSFA was performed first, and bone core biopsies were harvested at the time of staged implant placement to assess new bone formation. In the study by Avila-Ortiz

et al., a threshold RBH value of 4 mm was not correlated with vital bone formation $(18.7\% \pm 19.1\%$ vs. $22.3\% \pm 18.2\%$) (Avila-Ortiz et al. 2012). Pignaton et al. also reported that a threshold value of 2 mm did not negatively influence new bone formation $(26.2\% \pm 9.10\%$ vs. $29.8\% \pm 8.67\%$) (Pignaton et al. 2019). Those appear to align with the present study but still lack vital information regarding peri-implant bone formation due to the inevitable limitation in the timing of harvesting bone core biopsy specimens from human patients. However, %BIC and region-specific bone formation (which cannot be examined in clinical studies) in the present study provided further

TABLE 2 | Histomorphometric outcomes.

	Group SMT	Group STG	p	
Total augmentation				
TA (mm ²)	47.6 ± 6.9	48.8 ± 8.6	0.665	
$NB (mm^2)$	7.4 ± 1.8	8.0 ± 1.9	0.442	
$RM (mm^2)$	16.1 ± 1.8	14.4 ± 2.9	0.041	
FV (mm ²)	23.0 ± 5.6	25.3 ± 6.2	0.299	
%NB	15.7 ± 3.4	16.7 ± 4.0	0.326	
%RM	34.2 ± 5.0	29.8 ± 4.5	0.080	
%FV	47.6 ± 6.1	51.5 ± 5.1	0.101	
ROI_1				
Area of ROI ₁ (mm ²)	9.8 ± 1.1	9.3 ± 1.1	0.489	
$NB (mm^2)$	1.9 ± 0.5	1.7 ± 0.4	0.885	
$RM (mm^2)$	2.9 ± 0.8	2.6 ± 1.0	0.227	
FV (mm ²)	4.8 ± 0.8	4.8 ± 1.0	0.991	
%NB	19.8 ± 6.6	18.6 ± 5.8	0.547	
%RM	29.3 ± 6.5	27.5 ± 8.9	0.276	
%FV	48.8 ± 4.7	51.9 ± 7.3	0.213	
ROI_2				
Area of ROI ₂ (mm ²)	0.9 ± 0.3	0.9 ± 0.2	0.925	
$NB (mm^2)$	0.2 ± 0.1	0.2 ± 0.1	0.648	
$RM (mm^2)$	0.1 ± 0.1	0.1 ± 0.1	0.596	
FV (mm ²)	0.5 ± 0.2	0.5 ± 0.1	0.837	
%NB	25.9 ± 9.2	21.8 ± 13.2	0.358	
%RM	14.2 ± 11.8	15.2 ± 8.4	0.810	
%FV	55.2 ± 10.7	53.1 ± 12.4	0.615	
%Implant engagement	14.1 ± 1.8	13.7 ± 1.7	0.625	
%BIC	52.2 ± 16.6	44.9 ± 18.4	0.466	

Note: Data are mean ± standard-deviation.

Abbreviations: %FV, percentage of fibrovascular tissue in the respective region; %NB, percentage of newly formed bone in the respective region; %RM, percentage of residual bone substitute material in the respective region; FV, area of fibrovascular tissue; NB, area of newly formed bone; RM, area of residual bone substitute material; TA, area of total augmentation.

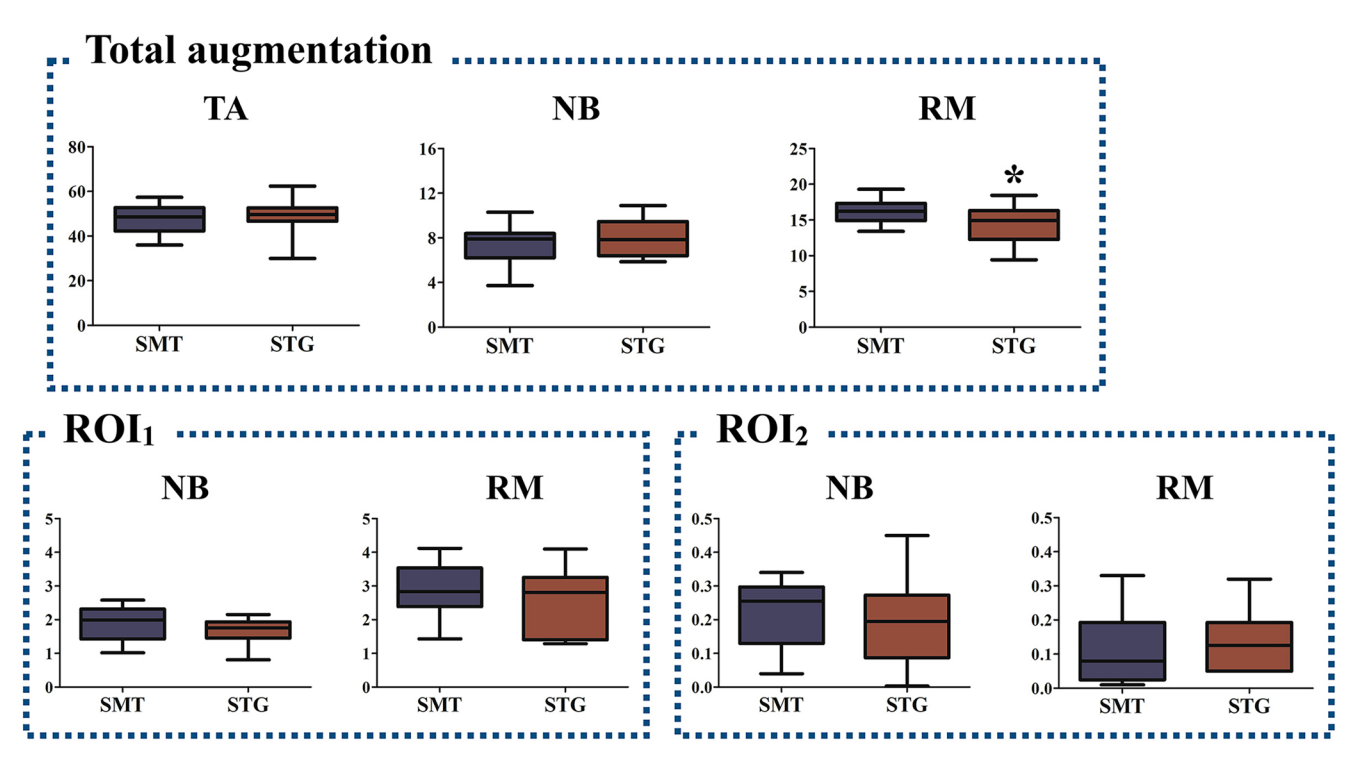


FIGURE 5 | Box plots presenting the results from the histomorphometric analyses. NB, area of newly formed bone; RM, area of residual bone substitute material; TA, Area of total augmentation; *Statistically significant difference between the groups.

evidence that RBH may not be the most substantial determinant, also enabling the capture of comprehensive pictures of peri-implant healing.

The primary stability of the implants should be addressed to understand the findings of the present study properly. Several studies have shown that micromotion of the implants could disrupt the bone formation process around the implant (Abdul-Kadir et al. 2008; Cameron et al. 1973; Cehreli et al. 2004; Szmukler-Moncler et al. 1998; Tobar-Reyes et al. 2021). Micromotion above a certain threshold (between 50 and 150 µm) may cause the formation of a fibrous layer on the implant surface, preventing bone formation directly on the implant surface. Thus, without proper primary stability, the present histomorphometric findings in group SMT could not be achieved. The macroscale design of implants influences the primary stability (Heimes et al. 2023). The tapered body and thread design of the implants in the present study favoured the attainment proper primary stability. Through this, the implants in group STG could get more time for bone apposition on the implant surface, especially through contact osteogenesis (Davies 2007). Notably, the %BIC was higher in group SMT compared to group STG albeit with no statistically significant difference. Bone conditions, such as the cortical bone plate and RBH, also influence primary stability (Han et al. 2016). The antral bone of the rabbit generally presents a well-developed cortical bone part, which can offer favourable initial implant stability. The percentage of implant engagement to the antral bone was small (14.1% in group SMT and 13.7% in group STG) because of the thin antral bone (approximately 0.7 mm in the present study) (Appendix 2). In the current model, such engagement ratios seemed acceptable not to transmit harmful force or micromotion along the implant.

The current experimental conditions, especially the thickness of the antral bone, may not be directly transferred to the clinical setting, but it suggests the feasibility of simultaneous implant placement with MSFA in the posterior maxilla with thin RBH. Still, in situations with an ill-developed cortical layer and requiring subcrestal implant placement, simultaneous implant placement is not viable.

In group STG, implant placement was performed 4weeks after MSFA. Based on the findings from rabbit sinus models, the ossification in the centre of the augmentation is usually slower compared to other regions (Lee et al. 2022; Lim et al. 2018; Sim et al. 2022). At 4weeks, the main tissue component at the centre of the augmentation encompasses a provisional matrix, immature woven bone and a small amount of lamellar bone. Osteotomy preparation at this stage seemed not to significantly interrupt the healing of immature tissue, considering the finding of ROI₂; but the drilling procedure made unconsolidated bone particles to leak out of the osteotomy hole. This yielded statistically significantly lower RM in group STG than in group SMT.

4.3 | The Current Animal Model

Various points should be clarified to understand the translational value of the present model. Appendix 3 presents such information.

4.4 | Limitations

There are several limitations to the present study. First, the group randomisation/allocation process in the present study carried a

high risk of bias (Ferreira and Patino 2016; McKenzie 2019). At least for the first experimental animal, randomisation could be applied even though coin-flipping is the least preferred method. However, from the second animal, the investigators had information about upcoming assignments, which could be a bias throughout the experiments. Block or adaptive randomisation should be considered to conceal the group allocation. Second, the sample size was arbitrarily determined based on a previous study (Thoma et al. 2018) because of the absence of prior research with similar topics. Alternative methods such as the resource equation method may be considered (Arifin and Zahiruddin 2017), which would indicate a sample size of 12. To address the limitations regarding sample size determination, a post hoc power calculation was additionally performed using the mean and standard deviation values of the primary outcome and an alpha level of 0.05 (G*Power version 3.1.9.7) (Faul et al. 2007), resulting in an effect size of 0.29 and a power of 13.3%. Considering the above two, further investigation using a larger sample is needed to confirm the current findings. Third, it may have been more informative to measure the implant stability value, considering the thinness of the antral bone.

5 | Conclusion

Simultaneous implant placement with MSFA might be a feasible treatment in the posterior maxilla with thin RBH, as suggested by radiographic and histomorphometric outcomes observed in this preclinical study. However, the simultaneous implant placement protocol should be cautiously implemented in situations where primary implant stability is achievable. While the present findings align with favourable outcomes in previous clinical studies on this specific topic, the current results should be cautiously interpreted within the context of an animal model.

Author Contributions

Ji-Youn Hong: analysis, writing – original draft preparation. Yeek Herr: analysis, interpretation, writing – original draft preparation. Nadja Naenni: analysis, interpretation. Daniel S. Thoma and Borvornwut Buranawat: critical revision. Seung-Il Shin: conception/design of the work, final approval of manuscript. Hyun-Chang Lim: conception/design of the work, investigation, critical revision.

Acknowledgements

We thank the research team of Department of Periodontology, Kyung Hee University College of Dentistry, Seoul, Korea. The experimental materials were kindly supplied by Dentium and Genoss.

Ethics Statement

The study protocol was approved by the Institutional Animal Research Committee at Kyung Hee Medical Center, Seoul, Korea (KHMC-IACUC 2022–038).

Conflicts of Interest

The authors declare no conflicts of interest.

Data Availability Statement

The data that support the findings of this study are available from the corresponding author upon reasonable request.

References

Abdul-Kadir, M. R., U. Hansen, R. Klabunde, D. Lucas, and A. Amis. 2008. "Finite Element Modelling of Primary Hip Stem Stability: The Effect of Interference Fit." *Journal of Biomechanics* 41: 587–594. https://doi.org/10.1016/j.jbiomech.2007.10.009.

Abuhussein, H., G. Pagni, A. Rebaudi, and H. L. Wang. 2010. "The Effect of Thread Pattern Upon Implant Osseointegration." *Clinical Oral Implants Research* 21: 129–136. https://doi.org/10.1111/j.1600-0501. 2009.01800.x.

Arifin, W. N., and W. M. Zahiruddin. 2017. "Sample Size Calculation in Animal Studies Using Resource Equation Approach." *Malaysian Journal of Medical Sciences* 24: 101–105. https://doi.org/10.21315/mjms2017.24.5.11.

Avila-Ortiz, G., R. Neiva, P. Galindo-Moreno, I. Rudek, E. Benavides, and H. L. Wang. 2012. "Analysis of the Influence of Residual Alveolar Bone Height on Sinus Augmentation Outcomes." *Clinical Oral Implants Research* 23: 1082–1088. https://doi.org/10.1111/j.1600-0501.2011.02270.x.

Baek, W. S., S. R. Yoon, H. C. Lim, J. S. Lee, S. H. Choi, and U. W. Jung. 2015. "Bone Formation Around rhBMP-2-Coated Implants in Rabbit Sinuses With or Without Absorbable Collagen Sponge Grafting." *Journal of Periodontal & Implant Science* 45: 238–246. https://doi.org/10.5051/jpis.2015.45.6.238.

Beck, F., K. M. Reich, S. Lettner, et al. 2021. "The Vertical Course of Bone Regeneration in Maxillary Sinus Floor Augmentations: A Histomorphometric Analysis of Human Biopsies." *Journal of Periodontology* 92: 263–272. https://doi.org/10.1002/JPER.19-0656.

Bernardello, F., D. Righi, F. Cosci, P. Bozzoli, C. M. Soardi, and S. Spinato. 2011. "Crestal Sinus Lift With Sequential Drills and Simultaneous Implant Placement in Sites With <5 Mm of Native Bone: A Multicenter Retrospective Study." *Implant Dentistry* 20: 439–444. https://doi.org/10.1097/ID.0b013e3182342052.

Cameron, H. U., R. M. Pilliar, and I. MacNab. 1973. "The Effect of Movement on the Bonding of Porous Metal to Bone." *Journal of Biomedical Materials Research* 7: 301–311. https://doi.org/10.1002/jbm. 820070404.

Cehreli, M., S. Sahin, and K. Akca. 2004. "Role of Mechanical Environment and Implant Design on Bone Tissue Differentiation: Current Knowledge and Future Contexts." *Journal of Dentistry* 32: 123–132. https://doi.org/10.1016/j.jdent.2003.09.003.

Corbella, S., S. Taschieri, and M. Del Fabbro. 2015. "Long-Term Outcomes for the Treatment of Atrophic Posterior Maxilla: A Systematic Review of Literature." *Clinical Implant Dentistry and Related Research* 17: 120–132. https://doi.org/10.1111/cid.12077.

Corbella, S., S. Taschieri, R. Weinstein, and M. Del Fabbro. 2016. "Histomorphometric Outcomes After Lateral Sinus Floor Elevation Procedure: A Systematic Review of the Literature and Meta-Analysis." *Clinical Oral Implants Research* 27: 1106–1122. https://doi.org/10.1111/clr.12702.

Davies, J. E. 2007. "Bone Bonding at Natural and Biomaterial Surfaces." *Biomaterials* 28: 5058–5067. https://doi.org/10.1016/j.biomaterials. 2007.07.049.

Del Fabbro, M., G. Rosano, and S. Taschieri. 2008. "Implant Survival Rates After Maxillary Sinus Augmentation." *European Journal of Oral Sciences* 116: 497–506. https://doi.org/10.1111/j.1600-0722.2008.

Del Fabbro, M., S. S. Wallace, and T. Testori. 2013. "Long-Term Implant Survival in the Grafted Maxillary Sinus: A Systematic Review." *International Journal of Periodontics and Restorative Dentistry* 33: 773–783. https://doi.org/10.11607/prd.1288.

Diefenbeck, M., T. Muckley, C. Schrader, et al. 2011. "The Effect of Plasma Chemical Oxidation of Titanium Alloy on Bone-Implant Contact in Rats." *Biomaterials* 32: 8041–8047. https://doi.org/10.1016/j.biomaterials.2011.07.046.

Faul, F., E. Erdfelder, A. G. Lang, and A. Buchner. 2007. "G*Power 3: A Flexible Statistical Power Analysis Program for the Social, Behavioral, and Biomedical Sciences." *Behavior Research Methods* 39: 175–191. https://doi.org/10.3758/bf03193146.

Ferreira, J. C., and C. M. Patino. 2016. "Randomization: Beyond Tossing a Coin." *Jornal Brasileiro de Pneumologia* 42: 310. https://doi.org/10.1590/S1806-37562016000000296.

Gonzalez, S., M. C. Tuan, K. M. Ahn, and H. Nowzari. 2014. "Crestal Approach for Maxillary Sinus Augmentation in Patients With </=4 Mm of Residual Alveolar Bone." *Clinical Implant Dentistry and Related Research* 16: 827–835. https://doi.org/10.1111/cid.12067.

Han, H. C., H. C. Lim, J. Y. Hong, et al. 2016. "Primary Implant Stability in a Bone Model Simulating Clinical Situations for the Posterior Maxilla: An In Vitro Study." *Journal of Periodontal & Implant Science* 46: 254–265. https://doi.org/10.5051/jpis.2016.46.4.254.

He, T., C. Cao, Z. Xu, et al. 2017. "A Comparison of Micro-CT and Histomorphometry for Evaluation of Osseointegration of PEO-Coated Titanium Implants in a Rat Model." *Scientific Reports* 7: 16270. https://doi.org/10.1038/s41598-017-16465-4.

Heimes, D., P. Becker, A. Pabst, et al. 2023. "How Does Dental Implant Macrogeometry Affect Primary Implant Stability? A Narrative Review." *International Journal of Implant Dentistry* 9: 20. https://doi.org/10.1186/s40729-023-00485-z.

Jamil, S. 2024. "Unlocking Implant Success: The Impact of Surgical Techniques on Primary Stability in the Posterior Maxilla." *Evidence-Based Dentistry* 25: 125–126. https://doi.org/10.1038/s41432-024-01051-1.

Jensen, O. T., L. B. Shulman, M. S. Block, and V. J. Iacono. 1998. "Report of the Sinus Consensus Conference of 1996." *International Journal of Oral & Maxillofacial Implants* 13, no. Suppl: 11–45.

Joo, M. J., J. K. Cha, H. C. Lim, S. H. Choi, and U. W. Jung. 2017. "Sinus Augmentation Using rhBMP-2-Loaded Synthetic Bone Substitute With Simultaneous Implant Placement in Rabbits." *Journal of Periodontal & Implant Science* 47: 86–95. https://doi.org/10.5051/jpis.2017.47.2.86.

Jung, U. W., O. Unursaikhan, J. Y. Park, J. S. Lee, J. Otgonbold, and S. H. Choi. 2015. "Tenting Effect of the Elevated Sinus Membrane Over an Implant With Adjunctive Use of a Hydroxyapatite-Powdered Collagen Membrane in Rabbits." *Clinical Oral Implants Research* 26: 663–670. https://doi.org/10.1111/clr.12362.

Kim, H. J., S. Yea, K. H. Kim, et al. 2020. "A Retrospective Study of Implants Placed Following 1-Stage or 2-Stage Maxillary Sinus Floor Augmentation by the Lateral Window Technique Performed on Residual Bone of <4 Mm: Results up to 10 Years of Follow-Up." *Journal of Periodontology* 91: 183–193. https://doi.org/10.1002/JPER.19-0066.

Kim, Y. S., S. H. Kim, K. H. Kim, et al. 2012. "Rabbit Maxillary Sinus Augmentation Model With Simultaneous Implant Placement: Differential Responses to the Graft Materials." *Journal of Periodontal & Implant Science* 42: 204–211. https://doi.org/10.5051/jpis.2012.

Lee, J. Y., S. Kim, S. Y. Shin, J. H. Chung, Y. Herr, and H. C. Lim. 2022. "Effectiveness of Hydraulic Pressure-Assisted Sinus Augmentation in a Rabbit Sinus Model: A Preclinical Study." *Clinical Oral Investigations* 26: 1581–1591. https://doi.org/10.1007/s00784-021-04131-z.

Lim, H. C., Y. Son, J. Y. Hong, S. I. Shin, U. W. Jung, and J. H. Chung. 2018. "Sinus Floor Elevation in Sites With a Perforated Schneiderian Membrane: What Is the Effect of Placing a Collagen Membrane in a Rabbit Model?" *Clinical Oral Implants Research* 29: 1202–1211. https://doi.org/10.1111/clr.13385.

Liu, Y., P. Ji, G. Fu, and H. Huang. 2022. "Transcrestal Sinus Augmentation With Simultaneous Implant Placement in 1 to $2\,\mathrm{Mm}$

Residual Alveolar Bone: A Case Report." *Journal of Oral Implantology* 48: 319–323. https://doi.org/10.1563/aaid-joi-D-20-00303.

Maniatopoulos, C., A. Rodriguez, D. A. Deporter, and A. H. Melcher. 1986. "An Improved Method for Preparing Histological Sections of Metallic Implants." *International Journal of Oral & Maxillofacial Implants* 1: 31–37.

Martins, S. H. L., U. B. Cadore, A. B. Novaes Jr., et al. 2022. "Evaluation of Bone Response to a Nano HA Implant Surface on Sinus Lifting Procedures: Study in Rabbits." *Journal of Functional Biomaterials* 13: 122. https://doi.org/10.3390/jfb13030122.

McKenzie, J. E. 2019. "Randomisation Is More Than a Coin Toss: The Role of Allocation Concealment." *BJOG: An International Journal of Obstetrics & Gynaecology* 126: 1288. https://doi.org/10.1111/1471-0528. 15559.

Peleg, M., G. Chaushu, Z. Mazor, L. Ardekian, and M. Bakoon. 1999. "Radiological Findings of the Post-Sinus Lift Maxillary Sinus: A Computerized Tomography Follow-Up." *Journal of Periodontology* 70: 1564–1573. https://doi.org/10.1902/jop.1999.70.12.1564.

Percie du Sert, N., V. Hurst, A. Ahluwalia, et al. 2020. "The ARRIVE Guidelines 2.0: Updated Guidelines for Reporting Animal Research." *PLoS Biology* 18: e3000410. https://doi.org/10.1371/journal.pbio. 3000410.

Pignaton, T. B., R. Spin-Neto, C. E. A. Ferreira, C. B. Martinelli, G. de Oliveira, and E. Marcantonio Jr. 2020. "Remodelling of Sinus Bone Grafts According to the Distance From the Native Bone: A Histomorphometric Analysis." *Clinical Oral Implants Research* 31: 959–967. https://doi.org/10.1111/clr.13639.

Pignaton, T. B., A. Wenzel, C. E. A. Ferreira, et al. 2019. "Influence of Residual Bone Height and Sinus Width on the Outcome of Maxillary Sinus Bone Augmentation Using Anorganic Bovine Bone." *Clinical Oral Implants Research* 30: 315–323. https://doi.org/10.1111/clr.13417.

Rosen, P. S., R. Summers, J. R. Mellado, et al. 1999. "The Bone-Added Osteotome Sinus Floor Elevation Technique: Multicenter Retrospective Report of Consecutively Treated Patients." *International Journal of Oral & Maxillofacial Implants* 14: 853–858.

Sim, J. E., S. Kim, J. Y. Hong, S. I. Shin, J. H. Chung, and H. C. Lim. 2022. "Effect of the Size of the Bony Access Window and the Collagen Barrier Over the Window in Sinus Floor Elevation: A Preclinical Investigation in a Rabbit Sinus Model." *Journal of Periodontal & Implant Science* 52: 325–337. https://doi.org/10.5051/jpis.2105560278.

Stubinger, S., and M. Dard. 2013. "The Rabbit as Experimental Model for Research in Implant Dentistry and Related Tissue Regeneration." *Journal of Investigative Surgery* 26: 266–282. https://doi.org/10.3109/08941939.2013.778922.

Szmukler-Moncler, S., H. Salama, Y. Reingewirtz, and J. H. Dubruille. 1998. "Timing of Loading and Effect of Micromotion on Bone-Dental Implant Interface: Review of Experimental Literature." *Journal of Biomedical Materials Research* 43: 192–203. https://doi.org/10.1002/(sici)1097-4636(199822)43:2<192::aid-jbm14>3.0.co;2-k.

Tabassum, A., G. J. Meijer, J. G. Wolke, and J. A. Jansen. 2010. "Influence of Surgical Technique and Surface Roughness on the Primary Stability of an Implant in Artificial Bone With Different Cortical Thickness: A Laboratory Study." *Clinical Oral Implants Research* 21: 213–220. https://doi.org/10.1111/j.1600-0501.2009.01823.x.

Thoma, D. S., S. R. Yoon, J. K. Cha, et al. 2018. "Sinus Floor Elevation Using Implants Coated With Recombinant Human Bone Morphogenetic Protein-2: Micro-Computed Tomographic and Histomorphometric Analyses." *Clinical Oral Investigations* 22: 829–837. https://doi.org/10.1007/s00784-017-2158-3.

Tobar-Reyes, J., L. Andueza-Castro, A. Jimenez-Silva, R. Bustamante-Plaza, and J. Carvajal-Herrera. 2021. "Micromotion Analysis of Immediately Loaded Implants With Titanium and Cobalt-Chrome Superstructures. 3D Finite Element Analysis." *Cllinical and*

Experimental Dental Research 7: 581–590. https://doi.org/10.1002/cre2.365.

Virnik, S., L. Cueni, and A. Kloss-Brandstatter. 2023. "Is One-Stage Lateral Sinus Lift and Implantation Safe in Severely Atrophic Maxillae? Results of a Comparative Pilot Study." *International Journal of Implant Dentistry* 9: 6. https://doi.org/10.1186/s40729-023-00471-5.

Wallace, S. S., and S. J. Froum. 2003. "Effect of Maxillary Sinus Augmentation on the Survival of Endosseous Dental Implants. A Systematic Review." *Annals of Periodontology* 8: 328–343. https://doi.org/10.1902/annals.2003.8.1.328.

Zhou, W., F. Wang, M. Magic, M. Zhuang, J. Sun, and Y. Wu. 2021. "The Effect of Anatomy on Osteogenesis After Maxillary Sinus Floor Augmentation: A Radiographic and Histological Analysis." *Clinical Oral Investigations* 25: 5197–5204. https://doi.org/10.1007/s00784-021-03827-6.

Appendix 1

Details of Materials and Methods

Animal Care and Handling

Ten male adult New Zealand white rabbits (weighing 2.5–3.0kg, 12 months old) were used. They were provided individual cages, a standard laboratory pellet diet and ad libitum access to water. Animals were monitored by a veterinarian. Intramuscular injection of an analgesic (ketoprofen 0.3 mL, Ketopro, Unibiotech, Anyang, Korea) and an antibiotic (gentamycin, 0.3 mL; Komi Gentamicin, Komipharm, Siheung, Korea) was administered postoperatively for 3 days.

One surgeon (H.-C. L.) performed all surgeries. A mixture of Zoletil 50 (tiletamine hydrochloride + zolazepam hydrochloride; Virbac S.A, Virbac Laboratories 06516, Carros, France) and Rompun (xylazine hydrochloride; Bayer, Seoul, Korea) was intramuscularly injected to induce general anaesthesia. The surgical sites were shaved and disinfected with iodine solution. Then, a local anaesthesia was administered using 2% lidocaine HCl containing 1:100,000 epinephrine (Huons, Seoul). The surgical protocol in the present study was a modified version of the previous studies (Baek et al. 2015; Joo et al. 2017; Thoma et al. 2018).

Group Allocation

For the first animal, group assignment to one of the sinuses was randomly determined by flipping a coin. Thereafter, the groups were allotted alternatively to the remaining animals.

Establishment of Regions of Interest in Micro-CT

Two regions of interest (ROIs) were established. The first ROI (ROI₁) was a conventional one, defined by the inner surface of the antral bone and the outline of a mixture of newly formed bone/residual bone substitute material with the exclusion of the implant. The second ROI (ROI₂) was a circular band around the implant between 60 and $375\,\mu m$ from the implant surface and an alternative to the bone-to-implant contact (Diefenbeck et al. 2011; He et al. 2017; Maniatopoulos et al. 1986). It has been demonstrated that the distance of 60 µm from the implant was sufficient to minimise artefacts from the metal (Diefenbeck et al. 2011). The outer boundary (set at 375 µm from the implant) of the second ROI was chosen because 25% of the radius of the implant has been a commonly applied distance (Maniatopoulos et al. 1986). Total augmented volume (TV; mm3) and the volumes of newly formed bone (NV; mm3) and residual bone substitute material (RV; mm3) were measured in ROI1. In ROI2, NV and RV were measured. The grey scales for newly formed bone and bone substitute materials were between 32 and 47 and between 48 and 80, respectively.

Histological Processing

After micro-CT, the retrieved specimens were dehydrated and resinembedded/polymerised using a specific system (Technovit 7200 VLC,

Kulzer GmbH, Wehrheim Germany). Then, the specimens were cut (EXAKT300, EXAKT Advanced Technologies GmbH, Norderstedt, Germnay), followed by grinding (EXAKT400CS, EXAKT Advanced Technologies GmbH) to obtain the section including the long axis of the implant. The thickness of the final histologic section was 70– $100\,\mu m$. Then, hematoxylin and eosin (H&E) staining was performed.

Training and Calibration of the Examiner

Before the main histomorphometric analysis was performed, an independent investigator (J.-Y., H.) was trained and calibrated using histological images from previous studies. In two sessions (at 1-week interval) of measuring five samples, intraclass correlation coefficients (ICCs) ranged between 0.915 and 0.982 (p < 0.05).

Sample Size Calculation

For determining the sample size, there was no previous study dealing with a similar topic in a rabbit sinus model. Therefore, we referred to the studies involving implant placement in rabbit sinuses. In those studies, the numbers of the experimental sites for one group at one healing timepoint were between 5 and 10 (Baek et al. 2015; Joo et al. 2017; Jung et al. 2015; Kim et al. 2012; Martins et al. 2022; Thoma et al. 2018). Based on this, the sample size in the present study was arbitrarily determined to be 10 animals.

Appendix 2

Antral Bone Thickness and Percentage of Implant Engagement to the Antral Bone

The mean thickness of the antral bone was not statistically significantly different between the two groups $(0.7\pm0.1\,\mathrm{mm}$ for both groups, p>0.05). This thickness was comparable to that measured clinically in a previous study $(0.6\pm0.1\,\mathrm{mm})$ (Jung et al. 2015). The percentage of engagement was $14.1\%\pm1.8\%$ in group SMT and $13.7\%\pm1.7\%$ in group STG (p>0.05).

Appendix 3

Current Animal Model

Comparisons to Studies With Rabbit Sinus Model Involving Implant Placement

In some preclinical studies using a rabbit sinus model, implant placement was performed to evaluate specific treatment for graftless MSFA (Baek et al. 2015; Jung et al. 2015; Thoma et al. 2018) and specific implant surfaces with/without bone grafting (Baek et al. 2015; Joo et al. 2017; Thoma et al. 2018; Martins et al. 2022). The diameter of the implants in those studies was 3 mm and the length was in a range of 4-6 mm. In all studies, no implant failure was reported like the present study, which suggests that the antral bone provides sufficient anchorage of the implants for primary implant stability. In those studies, new bone formation was evaluated using various parameters, such as the area of newly formed bone, new bone height and %BIC. Moreover, different regions of interest were established for further supporting the treatment outcomes in the studies, such as rectangular area along the lateral surfaces of the implant and the area between the implant threads. Three of those studies presented %BIC: 32.2% (with bone morphogenetic protein-2 coated implants) and 27.7% (with non-coated implants) at 8 weeks (Thoma et al. 2018); between 25% and 45% at 8 weeks (Baek et al. 2015); and 51.6% (with nano-hydroxyapatite surface implants) and 37.2% (with double acid-etched surface implants) at 60 days (Martins et al. 2022).

The surgical protocol of the present study was modified from the previous studies (Baek et al. 2015; Jung et al. 2015; Joo et al. 2017; Thoma et al. 2018). The decision on the size of the bony access window in a rabbit sinus model was dependent on the easiness of sinus membrane elevation. In the present study, the diameter of the window (3.7 mm) could be reduced compared to the previous studies (5.5 mm) because hydraulic pressure could ease sinus membrane elevation to the area for the implant (Lee et al. 2022; Sim et al. 2022). In most studies regarding

implant placement in the rabbit sinus (including the present one) (Baek et al. 2015; Joo et al. 2017; Thoma et al. 2018), the implant osteotomy hole was separately created anteriorly to the window border, but the distance between the window and osteotomy hole was set to be narrower in the present study $(1.0-1.5\,\mathrm{mm})$ than in the previous studies $(3\,\mathrm{mm})$. Through the above, the implants could be placed as centrally as possible in the sinus.

Considerations for the Current Experimental Model

In order to understand the translational value of the present study and understand the current experimental model, the following should be considered. First, different healing periods were chosen for the groups SMT (12weeks) and STG (8weeks) after implant placement despite the same total experimental period (12 weeks). To allow for the same healing period for osseointegration to both groups, one more surgery should have been planned, but this would have increased the morbidity in the experimental animals. From the authors' experience, more than two surgeries on rabbits significantly influence the mortality. It should be noted that the total treatment period is also a crucial clinical factor. Second, 4 weeks of healing after bone augmentation may be considered too early for implant placement compared to the clinical situation. From the literature, 4 weeks in rabbits roughly corresponds to 2-4 months in humans (Peleg et al. 1999). However, considering that endo-sinus bone formation is the most active near the antral bone (Lim et al. 2018; Lee et al. 2022; Sim et al. 2022), implant placement at this timepoint can be regarded as a feasible option in the rabbit sinus. Third, two osteotomy holes were made on the same bone plane, which differs from the clinical situation. Two osteotomy holes also might hamper bone regeneration. However, creating two osteotomy holes is experimentally more suitable to predictably achieve both sinus membrane elevation/bone graft material insertion and implant stability. The bony access window should be over a certain size enough to ease sinus membrane elevation (even though hydraulic presssure was applied in the present study). On the other hand, the implant osteotomy tends to be smaller than the access window because an implant diameter as small as possible is preferable for the rabbit sinus considering the dimension of the rabbit sinus. This necessitates two separate osteotomy holes. Fourth, the current sinus model in rabbits was not an exact replica of the human sinus for either lateral or transcrestal MSFA, because both the access window and implant osteotomy hole were made on the roof of the sinus and the spatial relationship between the sinus membrane and implant/bone substitute material was contrary to the clinical situation (Stubinger and Dard 2013). In one study, a similar surgical approach (to humans) was applied to the rabbit sinus, but this required invasive surgery, yet small accessibility (Kim et al. 2012). Thus, the current model can be interpreted as a representative of sinus floor elevation itself, irrespective of specifically lateral or transcrestal MSFA.

Despite the aforementioned limitations and differences from clinical situations, the rabbit sinus model offers relatively homogeneous anatomic conditions, such as the absence of sinus septum and consistent thickness of the antral bone. These features allow for more rigorous control of variables, which cannot be often standardised in clinical settings (even in clinical trials). Moreover, this enables obtaining more controlled data on a specific biological phenomenon.